

Measurements of the Branching Fractions of

$$B^0 \rightarrow K^{*0} K^+ K^-, B^0 \rightarrow K^{*0} \pi^+ K^-, B^0 \rightarrow K^{*0} K^+ \pi^-, \text{ and } B^0 \rightarrow K^{*0} \pi^+ \pi^-$$

B. Aubert,¹ M. Bona,¹ D. Boutigny,¹ Y. Karyotakis,¹ J. P. Lees,¹ V. Poireau,¹ X. Prudent,¹ V. Tisserand,¹
 A. Zghiche,¹ J. Garra Tico,² E. Grauges,² L. Lopez,³ A. Palano,³ M. Pappagallo,³ G. Eigen,⁴ B. Stugu,⁴
 L. Sun,⁴ G. S. Abrams,⁵ M. Battaglia,⁵ D. N. Brown,⁵ J. Button-Shafer,⁵ R. N. Cahn,⁵ Y. Groysman,⁵
 R. G. Jacobsen,⁵ J. A. Kadyk,⁵ L. T. Kerth,⁵ Yu. G. Kolomensky,⁵ G. Kukartsev,⁵ D. Lopes Pegna,⁵ G. Lynch,⁵
 L. M. Mir,⁵ T. J. Orimoto,⁵ I. L. Osipenkov,⁵ M. T. Ronan,^{5,*} K. Tackmann,⁵ T. Tanabe,⁵ W. A. Wenzel,⁵
 P. del Amo Sanchez,⁶ C. M. Hawkes,⁶ A. T. Watson,⁶ H. Koch,⁷ T. Schroeder,⁷ D. Walker,⁸ D. J. Asgeirsson,⁹
 T. Cuhadar-Donszelmann,⁹ B. G. Fulsom,⁹ C. Hearty,⁹ T. S. Mattison,⁹ J. A. McKenna,⁹ A. Khan,¹⁰ M. Saleem,¹⁰
 L. Teodorescu,¹⁰ V. E. Blinov,¹¹ A. D. Bukin,¹¹ V. P. Druzhinin,¹¹ V. B. Golubev,¹¹ A. P. Onuchin,¹¹
 S. I. Serednyakov,¹¹ Yu. I. Skovpen,¹¹ E. P. Solodov,¹¹ K. Yu. Todyshev,¹¹ M. Bondioli,¹² S. Curry,¹² I. Eschrich,¹²
 D. Kirkby,¹² A. J. Lankford,¹² P. Lund,¹² M. Mandelkern,¹² E. C. Martin,¹² D. P. Stoker,¹² S. Abachi,¹³
 C. Buchanan,¹³ S. D. Foulkes,¹⁴ J. W. Gary,¹⁴ F. Liu,¹⁴ O. Long,¹⁴ B. C. Shen,¹⁴ G. M. Vitug,¹⁴ L. Zhang,¹⁴
 H. P. Paar,¹⁵ S. Rahatlou,¹⁵ V. Sharma,¹⁵ J. W. Berryhill,¹⁶ C. Campagnari,¹⁶ A. Cunha,¹⁶ B. Dahmes,¹⁶
 T. M. Hong,¹⁶ D. Kovalskyi,¹⁶ J. D. Richman,¹⁶ T. W. Beck,¹⁷ A. M. Eisner,¹⁷ C. J. Flacco,¹⁷ C. A. Heusch,¹⁷
 J. Kroseberg,¹⁷ W. S. Lockman,¹⁷ T. Schalk,¹⁷ B. A. Schumm,¹⁷ A. Seiden,¹⁷ M. G. Wilson,¹⁷ L. O. Winstrom,¹⁷
 E. Chen,¹⁸ C. H. Cheng,¹⁸ F. Fang,¹⁸ D. G. Hitlin,¹⁸ I. Narsky,¹⁸ T. Piatenko,¹⁸ F. C. Porter,¹⁸ R. Andreassen,¹⁹
 G. Mancinelli,¹⁹ B. T. Meadows,¹⁹ K. Mishra,¹⁹ M. D. Sokoloff,¹⁹ F. Blanc,²⁰ P. C. Bloom,²⁰ S. Chen,²⁰
 W. T. Ford,²⁰ J. F. Hirschauer,²⁰ A. Kreisel,²⁰ M. Nagel,²⁰ U. Nauenberg,²⁰ A. Olivas,²⁰ J. G. Smith,²⁰
 K. A. Ulmer,²⁰ S. R. Wagner,²⁰ J. Zhang,²⁰ A. M. Gabareen,²¹ A. Soffer,^{21,†} W. H. Toki,²¹ R. J. Wilson,²¹
 F. Winklmeier,²¹ D. D. Altenburg,²² E. Feltresi,²² A. Hauke,²² H. Jasper,²² J. Merkel,²² A. Petzold,²² B. Spaan,²²
 K. Wacker,²² V. Klose,²³ M. J. Kobel,²³ H. M. Lacker,²³ W. F. Mader,²³ R. Nogowski,²³ J. Schubert,²³
 K. R. Schubert,²³ R. Schwierz,²³ J. E. Sundermann,²³ A. Volk,²³ D. Bernard,²⁴ G. R. Bonneaud,²⁴ E. Latour,²⁴
 V. Lombardo,²⁴ Ch. Thiebaux,²⁴ M. Verderi,²⁴ P. J. Clark,²⁵ W. Gradl,²⁵ F. Muheim,²⁵ S. Playfer,²⁵
 A. I. Robertson,²⁵ J. E. Watson,²⁵ Y. Xie,²⁵ M. Andreotti,²⁶ D. Bettoni,²⁶ C. Bozzi,²⁶ R. Calabrese,²⁶ A. Cecchi,²⁶
 G. Cibinetto,²⁶ P. Franchini,²⁶ E. Luppi,²⁶ M. Negrini,²⁶ A. Petrella,²⁶ L. Piemontese,²⁶ E. Prencipe,²⁶
 V. Santoro,²⁶ F. Anulli,²⁷ R. Baldini-Ferrolì,²⁷ A. Calcaterra,²⁷ R. de Sangro,²⁷ G. Finocchiaro,²⁷ S. Pacetti,²⁷
 P. Patteri,²⁷ I. M. Peruzzi,^{27,‡} M. Piccolo,²⁷ M. Rama,²⁷ A. Zallo,²⁷ A. Buzzo,²⁸ R. Contri,²⁸ M. Lo Vetere,²⁸
 M. M. Macri,²⁸ M. R. Monge,²⁸ S. Passaggio,²⁸ C. Patrignani,²⁸ E. Robutti,²⁸ A. Santroni,²⁸ S. Tosi,²⁸
 K. S. Chaisanguanthum,²⁹ M. Morii,²⁹ J. Wu,²⁹ R. S. Dubitzky,³⁰ J. Marks,³⁰ S. Schenk,³⁰ U. Uwer,³⁰ D. J. Bard,³¹
 P. D. Dauncey,³¹ R. L. Flack,³¹ J. A. Nash,³¹ W. Panduro Vazquez,³¹ M. Tibbetts,³¹ P. K. Behera,³² X. Chai,³²
 M. J. Charles,³² U. Mallik,³² J. Cochran,³³ H. B. Crawley,³³ L. Dong,³³ V. Eyges,³³ W. T. Meyer,³³ S. Prell,³³
 E. I. Rosenberg,³³ A. E. Rubin,³³ Y. Y. Gao,³⁴ A. V. Gritsan,³⁴ Z. J. Guo,³⁴ C. K. Lae,³⁴ A. G. Denig,³⁵
 M. Fritsch,³⁵ G. Schott,³⁵ N. Arnaud,³⁶ J. Béguilleux,³⁶ A. D'Orazio,³⁶ M. Davier,³⁶ G. Grosdidier,³⁶ A. Höcker,³⁶
 V. Lepeltier,³⁶ F. Le Diberder,³⁶ A. M. Lutz,³⁶ S. Pruvot,³⁶ S. Rodier,³⁶ P. Roudeau,³⁶ M. H. Schune,³⁶
 J. Serrano,³⁶ V. Sordini,³⁶ A. Stocchi,³⁶ W. F. Wang,³⁶ G. Wormser,³⁶ D. J. Lange,³⁷ D. M. Wright,³⁷ I. Bingham,³⁸
 J. P. Burke,³⁸ C. A. Chavez,³⁸ J. R. Fry,³⁸ E. Gabathuler,³⁸ R. Gamet,³⁸ D. E. Hutchcroft,³⁸ D. J. Payne,³⁸
 K. C. Schofield,³⁸ C. Touramanis,³⁸ A. J. Bevan,³⁹ K. A. George,³⁹ F. Di Lodovico,³⁹ R. Sacco,³⁹ G. Cowan,⁴⁰
 H. U. Flaecher,⁴⁰ D. A. Hopkins,⁴⁰ S. Paramesvaran,⁴⁰ F. Salvatore,⁴⁰ A. C. Wren,⁴⁰ D. N. Brown,⁴¹ C. L. Davis,⁴¹
 J. Allison,⁴² D. Bailey,⁴² N. R. Barlow,⁴² R. J. Barlow,⁴² Y. M. Chia,⁴² C. L. Edgar,⁴² G. D. Lafferty,⁴²
 T. J. West,⁴² J. I. Yi,⁴² J. Anderson,⁴³ C. Chen,⁴³ A. Jawahery,⁴³ D. A. Roberts,⁴³ G. Simi,⁴³ J. M. Tuggle,⁴³
 G. Blaylock,⁴⁴ C. Dallapiccola,⁴⁴ S. S. Hertzbach,⁴⁴ X. Li,⁴⁴ T. B. Moore,⁴⁴ E. Salvati,⁴⁴ S. Saremi,⁴⁴ R. Cowan,⁴⁵
 D. Dujmic,⁴⁵ P. H. Fisher,⁴⁵ K. Koeneké,⁴⁵ G. Sciolla,⁴⁵ M. Spitznagel,⁴⁵ F. Taylor,⁴⁵ R. K. Yamamoto,⁴⁵
 M. Zhao,⁴⁵ Y. Zheng,⁴⁵ S. E. McLaughlin,^{46,*} P. M. Patel,⁴⁶ S. H. Robertson,⁴⁶ A. Lazzaro,⁴⁷ F. Palombo,⁴⁷
 J. M. Bauer,⁴⁸ L. Cremaldi,⁴⁸ V. Eschenburg,⁴⁸ R. Godang,⁴⁸ R. Kroeger,⁴⁸ D. A. Sanders,⁴⁸ D. J. Summers,⁴⁸
 H. W. Zhao,⁴⁸ S. Brunet,⁴⁹ D. Côté,⁴⁹ M. Simard,⁴⁹ P. Taras,⁴⁹ F. B. Viaud,⁴⁹ H. Nicholson,⁵⁰ G. De Nardo,⁵¹
 F. Fabozzi,^{51,§} L. Lista,⁵¹ D. Monorchio,⁵¹ C. Sciacca,⁵¹ M. A. Baak,⁵² G. Raven,⁵² H. L. Snoek,⁵² C. P. Jessop,⁵³
 K. J. Knoepfel,⁵³ J. M. LoSecco,⁵³ G. Benelli,⁵⁴ L. A. Corwin,⁵⁴ K. Honscheid,⁵⁴ H. Kagan,⁵⁴ R. Kass,⁵⁴

J. P. Morris,⁵⁴ A. M. Rahimi,⁵⁴ J. J. Regensburger,⁵⁴ S. J. Sekula,⁵⁴ Q. K. Wong,⁵⁴ N. L. Blount,⁵⁵ J. Brau,⁵⁵ R. Frey,⁵⁵ O. Igonkina,⁵⁵ J. A. Kolb,⁵⁵ M. Lu,⁵⁵ R. Rahmat,⁵⁵ N. B. Sinev,⁵⁵ D. Strom,⁵⁵ J. Strube,⁵⁵ E. Torrence,⁵⁵ N. Gagliardi,⁵⁶ A. Gaz,⁵⁶ M. Margoni,⁵⁶ M. Morandin,⁵⁶ A. Pompili,⁵⁶ M. Posocco,⁵⁶ M. Rotondo,⁵⁶ F. Simonetto,⁵⁶ R. Stroili,⁵⁶ C. Voci,⁵⁶ E. Ben-Haim,⁵⁷ H. Briand,⁵⁷ G. Calderini,⁵⁷ J. Chauveau,⁵⁷ P. David,⁵⁷ L. Del Buono,⁵⁷ Ch. de la Vaissière,⁵⁷ O. Hamon,⁵⁷ Ph. Leruste,⁵⁷ J. Malclès,⁵⁷ J. Ocariz,⁵⁷ A. Perez,⁵⁷ J. Prendki,⁵⁷ L. Gladney,⁵⁸ M. Biasini,⁵⁹ R. Covarelli,⁵⁹ E. Manoni,⁵⁹ C. Angelini,⁶⁰ G. Batignani,⁶⁰ S. Bettarini,⁶⁰ M. Carpinelli,⁶⁰ R. Cenci,⁶⁰ A. Cervelli,⁶⁰ F. Forti,⁶⁰ M. A. Giorgi,⁶⁰ A. Lusiani,⁶⁰ G. Marchiori,⁶⁰ M. A. Mazur,⁶⁰ M. Morganti,⁶⁰ N. Neri,⁶⁰ E. Paoloni,⁶⁰ G. Rizzo,⁶⁰ J. J. Walsh,⁶⁰ J. Biesiada,⁶¹ P. Elmer,⁶¹ Y. P. Lau,⁶¹ C. Lu,⁶¹ J. Olsen,⁶¹ A. J. S. Smith,⁶¹ A. V. Telnov,⁶¹ E. Baracchini,⁶² F. Bellini,⁶² G. Cavoto,⁶² D. del Re,⁶² E. Di Marco,⁶² R. Faccini,⁶² F. Ferrarotto,⁶² F. Ferroni,⁶² M. Gaspero,⁶² P. D. Jackson,⁶² L. Li Gioi,⁶² M. A. Mazzoni,⁶² S. Morganti,⁶² G. Piredda,⁶² F. Polci,⁶² F. Renga,⁶² C. Voena,⁶² M. Ebert,⁶³ T. Hartmann,⁶³ H. Schröder,⁶³ R. Waldi,⁶³ T. Adye,⁶⁴ G. Castelli,⁶⁴ B. Franek,⁶⁴ E. O. Olaiya,⁶⁴ W. Roethel,⁶⁴ F. F. Wilson,⁶⁴ S. Emery,⁶⁵ M. Escalier,⁶⁵ A. Gaidot,⁶⁵ S. F. Ganzhur,⁶⁵ G. Hamel de Monchenault,⁶⁵ W. Kozanecki,⁶⁵ G. Vasseur,⁶⁵ Ch. Yèche,⁶⁵ M. Zito,⁶⁵ X. R. Chen,⁶⁶ H. Liu,⁶⁶ W. Park,⁶⁶ M. V. Purohit,⁶⁶ R. M. White,⁶⁶ J. R. Wilson,⁶⁶ M. T. Allen,⁶⁷ D. Aston,⁶⁷ R. Bartoldus,⁶⁷ P. Bechtle,⁶⁷ R. Claus,⁶⁷ J. P. Coleman,⁶⁷ M. R. Convery,⁶⁷ J. C. Dingfelder,⁶⁷ J. Dorfan,⁶⁷ G. P. Dubois-Felsmann,⁶⁷ W. Dunwoodie,⁶⁷ R. C. Field,⁶⁷ T. Glanzman,⁶⁷ S. J. Gowdy,⁶⁷ M. T. Graham,⁶⁷ P. Grenier,⁶⁷ C. Hast,⁶⁷ W. R. Innes,⁶⁷ J. Kaminski,⁶⁷ M. H. Kelsey,⁶⁷ H. Kim,⁶⁷ P. Kim,⁶⁷ M. L. Kocian,⁶⁷ D. W. G. S. Leith,⁶⁷ S. Li,⁶⁷ S. Luitz,⁶⁷ V. Luth,⁶⁷ H. L. Lynch,⁶⁷ D. B. MacFarlane,⁶⁷ H. Marsiske,⁶⁷ R. Messner,⁶⁷ D. R. Muller,⁶⁷ C. P. O'Grady,⁶⁷ I. Ofte,⁶⁷ A. Perazzo,⁶⁷ M. Perl,⁶⁷ T. Pulliam,⁶⁷ B. N. Ratcliff,⁶⁷ A. Roodman,⁶⁷ A. A. Salnikov,⁶⁷ R. H. Schindler,⁶⁷ J. Schwiening,⁶⁷ A. Snyder,⁶⁷ D. Su,⁶⁷ M. K. Sullivan,⁶⁷ K. Suzuki,⁶⁷ S. K. Swain,⁶⁷ J. M. Thompson,⁶⁷ J. Va'vra,⁶⁷ A. P. Wagner,⁶⁷ M. Weaver,⁶⁷ W. J. Wisniewski,⁶⁷ M. Wittgen,⁶⁷ D. H. Wright,⁶⁷ A. K. Yarritu,⁶⁷ K. Yi,⁶⁷ C. C. Young,⁶⁷ V. Ziegler,⁶⁷ P. R. Burchat,⁶⁸ A. J. Edwards,⁶⁸ S. A. Majewski,⁶⁸ T. S. Miyashita,⁶⁸ B. A. Petersen,⁶⁸ L. Wilden,⁶⁸ S. Ahmed,⁶⁹ M. S. Alam,⁶⁹ R. Bula,⁶⁹ J. A. Ernst,⁶⁹ V. Jain,⁶⁹ B. Pan,⁶⁹ M. A. Saeed,⁶⁹ F. R. Wappler,⁶⁹ S. B. Zain,⁶⁹ M. Krishnamurthy,⁷⁰ S. M. Spanier,⁷⁰ R. Eckmann,⁷¹ J. L. Ritchie,⁷¹ A. M. Ruland,⁷¹ C. J. Schilling,⁷¹ R. F. Schwitters,⁷¹ J. M. Izen,⁷² X. C. Lou,⁷² S. Ye,⁷² F. Bianchi,⁷³ F. Gallo,⁷³ D. Gamba,⁷³ M. Pelliccioni,⁷³ M. Bomben,⁷⁴ L. Bosio,⁷⁴ C. Cartaro,⁷⁴ F. Cossutti,⁷⁴ G. Della Ricca,⁷⁴ L. Lanceri,⁷⁴ L. Vitale,⁷⁴ V. Azzolini,⁷⁵ N. Lopez-March,⁷⁵ F. Martinez-Vidal,⁷⁵ D. A. Milanes,⁷⁵ A. Oyanguren,⁷⁵ J. Albert,⁷⁶ Sw. Banerjee,⁷⁶ B. Bhuyan,⁷⁶ K. Hamano,⁷⁶ R. Kowalewski,⁷⁶ I. M. Nugent,⁷⁶ J. M. Roney,⁷⁶ R. J. Sobie,⁷⁶ P. F. Harrison,⁷⁷ J. Ilic,⁷⁷ T. E. Latham,⁷⁷ G. B. Mohanty,⁷⁷ H. R. Band,⁷⁸ X. Chen,⁷⁸ S. Dasu,⁷⁸ K. T. Flood,⁷⁸ J. J. Hollar,⁷⁸ P. E. Kutter,⁷⁸ Y. Pan,⁷⁸ M. Pierini,⁷⁸ R. Prepost,⁷⁸ S. L. Wu,⁷⁸ and H. Neal⁷⁹

(The BABAR Collaboration)

¹Laboratoire de Physique des Particules, IN2P3/CNRS et Université de Savoie, F-74941 Annecy-Le-Vieux, France

²Universitat de Barcelona, Facultat de Física, Departament ECM, E-08028 Barcelona, Spain

³Università di Bari, Dipartimento di Fisica and INFN, I-70126 Bari, Italy

⁴University of Bergen, Institute of Physics, N-5007 Bergen, Norway

⁵Lawrence Berkeley National Laboratory and University of California, Berkeley, California 94720, USA

⁶University of Birmingham, Birmingham, B15 2TT, United Kingdom

⁷Ruhr Universität Bochum, Institut für Experimentalphysik 1, D-44780 Bochum, Germany

⁸University of Bristol, Bristol BS8 1TL, United Kingdom

⁹University of British Columbia, Vancouver, British Columbia, Canada V6T 1Z1

¹⁰Brunel University, Uxbridge, Middlesex UB8 3PH, United Kingdom

¹¹Budker Institute of Nuclear Physics, Novosibirsk 630090, Russia

¹²University of California at Irvine, Irvine, California 92697, USA

¹³University of California at Los Angeles, Los Angeles, California 90024, USA

¹⁴University of California at Riverside, Riverside, California 92521, USA

¹⁵University of California at San Diego, La Jolla, California 92093, USA

¹⁶University of California at Santa Barbara, Santa Barbara, California 93106, USA

¹⁷University of California at Santa Cruz, Institute for Particle Physics, Santa Cruz, California 95064, USA

¹⁸California Institute of Technology, Pasadena, California 91125, USA

¹⁹University of Cincinnati, Cincinnati, Ohio 45221, USA

²⁰University of Colorado, Boulder, Colorado 80309, USA

²¹Colorado State University, Fort Collins, Colorado 80523, USA

²²Universität Dortmund, Institut für Physik, D-44221 Dortmund, Germany

²³Technische Universität Dresden, Institut für Kern- und Teilchenphysik, D-01062 Dresden, Germany

²⁴Laboratoire Leprince-Ringuet, CNRS/IN2P3, Ecole Polytechnique, F-91128 Palaiseau, France

- ²⁵University of Edinburgh, Edinburgh EH9 3JZ, United Kingdom
- ²⁶Università di Ferrara, Dipartimento di Fisica and INFN, I-44100 Ferrara, Italy
- ²⁷Laboratori Nazionali di Frascati dell'INFN, I-00044 Frascati, Italy
- ²⁸Università di Genova, Dipartimento di Fisica and INFN, I-16146 Genova, Italy
- ²⁹Harvard University, Cambridge, Massachusetts 02138, USA
- ³⁰Universität Heidelberg, Physikalisches Institut, Philosophenweg 12, D-69120 Heidelberg, Germany
- ³¹Imperial College London, London, SW7 2AZ, United Kingdom
- ³²University of Iowa, Iowa City, Iowa 52242, USA
- ³³Iowa State University, Ames, Iowa 50011-3160, USA
- ³⁴Johns Hopkins University, Baltimore, Maryland 21218, USA
- ³⁵Universität Karlsruhe, Institut für Experimentelle Kernphysik, D-76021 Karlsruhe, Germany
- ³⁶Laboratoire de l'Accélérateur Linéaire, IN2P3/CNRS et Université Paris-Sud 11, Centre Scientifique d'Orsay, B. P. 34, F-91898 ORSAY Cedex, France
- ³⁷Lawrence Livermore National Laboratory, Livermore, California 94550, USA
- ³⁸University of Liverpool, Liverpool L69 7ZE, United Kingdom
- ³⁹Queen Mary, University of London, E1 4NS, United Kingdom
- ⁴⁰University of London, Royal Holloway and Bedford New College, Egham, Surrey TW20 0EX, United Kingdom
- ⁴¹University of Louisville, Louisville, Kentucky 40292, USA
- ⁴²University of Manchester, Manchester M13 9PL, United Kingdom
- ⁴³University of Maryland, College Park, Maryland 20742, USA
- ⁴⁴University of Massachusetts, Amherst, Massachusetts 01003, USA
- ⁴⁵Massachusetts Institute of Technology, Laboratory for Nuclear Science, Cambridge, Massachusetts 02139, USA
- ⁴⁶McGill University, Montréal, Québec, Canada H3A 2T8
- ⁴⁷Università di Milano, Dipartimento di Fisica and INFN, I-20133 Milano, Italy
- ⁴⁸University of Mississippi, University, Mississippi 38677, USA
- ⁴⁹Université de Montréal, Physique des Particules, Montréal, Québec, Canada H3C 3J7
- ⁵⁰Mount Holyoke College, South Hadley, Massachusetts 01075, USA
- ⁵¹Università di Napoli Federico II, Dipartimento di Scienze Fisiche and INFN, I-80126, Napoli, Italy
- ⁵²NIKHEF, National Institute for Nuclear Physics and High Energy Physics, NL-1009 DB Amsterdam, The Netherlands
- ⁵³University of Notre Dame, Notre Dame, Indiana 46556, USA
- ⁵⁴Ohio State University, Columbus, Ohio 43210, USA
- ⁵⁵University of Oregon, Eugene, Oregon 97403, USA
- ⁵⁶Università di Padova, Dipartimento di Fisica and INFN, I-35131 Padova, Italy
- ⁵⁷Laboratoire de Physique Nucléaire et de Hautes Energies, IN2P3/CNRS, Université Pierre et Marie Curie-Paris6, Université Denis Diderot-Paris7, F-75252 Paris, France
- ⁵⁸University of Pennsylvania, Philadelphia, Pennsylvania 19104, USA
- ⁵⁹Università di Perugia, Dipartimento di Fisica and INFN, I-06100 Perugia, Italy
- ⁶⁰Università di Pisa, Dipartimento di Fisica, Scuola Normale Superiore and INFN, I-56127 Pisa, Italy
- ⁶¹Princeton University, Princeton, New Jersey 08544, USA
- ⁶²Università di Roma La Sapienza, Dipartimento di Fisica and INFN, I-00185 Roma, Italy
- ⁶³Universität Rostock, D-18051 Rostock, Germany
- ⁶⁴Rutherford Appleton Laboratory, Chilton, Didcot, Oxon, OX11 0QX, United Kingdom
- ⁶⁵DSM/Dapnia, CEA/Saclay, F-91191 Gif-sur-Yvette, France
- ⁶⁶University of South Carolina, Columbia, South Carolina 29208, USA
- ⁶⁷Stanford Linear Accelerator Center, Stanford, California 94309, USA
- ⁶⁸Stanford University, Stanford, California 94305-4060, USA
- ⁶⁹State University of New York, Albany, New York 12222, USA
- ⁷⁰University of Tennessee, Knoxville, Tennessee 37996, USA
- ⁷¹University of Texas at Austin, Austin, Texas 78712, USA
- ⁷²University of Texas at Dallas, Richardson, Texas 75083, USA
- ⁷³Università di Torino, Dipartimento di Fisica Sperimentale and INFN, I-10125 Torino, Italy
- ⁷⁴Università di Trieste, Dipartimento di Fisica and INFN, I-34127 Trieste, Italy
- ⁷⁵IFIC, Universitat de Valencia-CSIC, E-46071 Valencia, Spain
- ⁷⁶University of Victoria, Victoria, British Columbia, Canada V8W 3P6
- ⁷⁷Department of Physics, University of Warwick, Coventry CV4 7AL, United Kingdom
- ⁷⁸University of Wisconsin, Madison, Wisconsin 53706, USA
- ⁷⁹Yale University, New Haven, Connecticut 06511, USA
- (Dated: June 2, 2008)

Branching fraction measurements of charmless $B^0 \rightarrow K^{*0} h_1^+ h_2^-$ ($h_{1,2} = K, \pi$) decays are presented, using a data sample of 383 million $\Upsilon(4S) \rightarrow B\bar{B}$ decays collected with the BABAR detector at the PEP-II asymmetric-energy B -meson factory at SLAC. The results are: $\mathcal{B}(B^0 \rightarrow K^{*0} K^+ K^-) = (27.5 \pm 1.3 \pm 2.2) \times 10^{-6}$, $\mathcal{B}(B^0 \rightarrow K^{*0} \pi^+ K^-) = (4.6 \pm 1.1 \pm 0.8) \times 10^{-6}$ and $\mathcal{B}(B^0 \rightarrow$

$K^{*0}\pi^+\pi^- = (54.5 \pm 2.9 \pm 4.3) \times 10^{-6}$. The first errors quoted are statistical and the second are systematic. An upper limit is set for $\mathcal{B}(B^0 \rightarrow K^{*0}K^+\pi^-) < 2.2 \times 10^{-6}$ at 90% confidence level. We also present measurements of CP -violating asymmetries for the observed decays.

PACS numbers: 13.25.Hw, 12.15.Hh, 11.30.Er

Charmless decays of B mesons to three-body final states are important probes of the weak interaction and the complex quark couplings of the Cabibbo–Kobayashi–Maskawa (CKM) matrix [1]. Improved experimental measurements of these charmless decays, combined with theoretical developments, can provide significant constraints on the CKM matrix elements and potentially uncover evidence for physics beyond the Standard Model. For example, the branching fraction of the decay $B^0 \rightarrow K^{*0}\pi^+K^-$ is sensitive to the CKM matrix elements V_{td} and V_{ub} (see Fig. 1). Additionally, a branching fraction of the Standard Model suppressed decay $B^0 \rightarrow K^{*0}K^+\pi^-$ comparable or larger than that of $B^0 \rightarrow K^{*0}\pi^+K^-$ would be an indication of new physics.

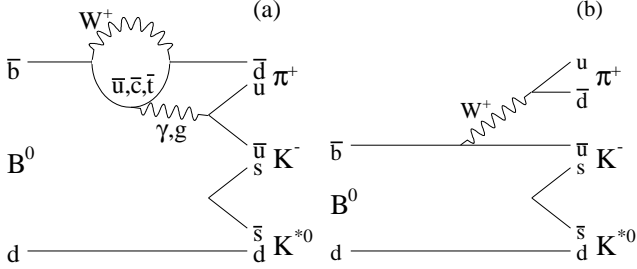


FIG. 1: (a) Penguin and (b) tree Feynman diagrams for the decay $B^0 \rightarrow K^{*0}\pi^+K^-$. Similar Standard Model diagrams do not exist for the $\Delta S = 2$ decay $B^0 \rightarrow K^{*0}K^+\pi^-$.

Neutral B -meson decays to $K^+\pi^-h_1^+h_2^-$ (where $h_{1,2} = K$ or π) are dominated by $K^{*0}h_1^+h_2^-$, but can also proceed via a four-body nonresonant component, through intermediate charmless resonances such as $B^0 \rightarrow K^{*0}\phi$ or $B^0 \rightarrow K^{*0}\rho^0$ [2, 3, 4], or other as-yet-unobserved intermediate charmless resonances. To date, there are only limits on the inclusive decays $B^0 \rightarrow K^{*0}h_1^+h_2^-$, measured by the ARGUS experiment using less than 0.2 fb^{-1} [5], whilst there are more accurate measurements of charged B -meson decays to $K^{*+}h_1^+h_2^-$ [6].

We identify K^{*0} mesons through their decay to $K^+\pi^-$; consequently, the states $B^0 \rightarrow K^{*0}h_1^+h_2^-$ are self-tagged as the charge of the daughter kaon from the K^* reflects the flavor of the B^0 meson. The CP -violating decay rate asymmetry is defined as

$$\mathcal{A}_{K^*h_1h_2} \equiv \frac{\Gamma_{\bar{K}^{*0}h_1^-h_2^+} - \Gamma_{K^{*0}h_1^+h_2^-}}{\Gamma_{\bar{K}^{*0}h_1^-h_2^+} + \Gamma_{K^{*0}h_1^+h_2^-}}, \quad (1)$$

where Γ is the partial B decay width.

In this paper, branching fractions of $B^0 \rightarrow K^{*0}K^+K^-$, $B^0 \rightarrow K^{*0}\pi^+K^-$ and $B^0 \rightarrow K^{*0}\pi^+\pi^-$ are measured, and an upper limit is set for the Standard Model suppressed decay $B^0 \rightarrow K^{*0}K^+\pi^-$ [7]. The selection criteria require events with a reconstructed $K^+\pi^-h_1^+h_2^-$ final state, so that the total charmless contribution (including resonant charmless substructure) to the $K^{*0}h_1^+h_2^-$ Dalitz plot can be measured. The $\mathcal{A}_{K^*h_1h_2}$ values for the observed decays $B^0 \rightarrow K^{*0}K^+K^-$, $B^0 \rightarrow K^{*0}\pi^+K^-$, and $B^0 \rightarrow K^{*0}\pi^+\pi^-$ are also measured.

The data on which this analysis is based were collected with the BABAR detector [8] at the PEP-II asymmetric-energy e^+e^- storage ring. The BABAR detector consists of a double-sided five-layer silicon tracker, a 40-layer drift chamber, a Cherenkov detector, an electromagnetic calorimeter, and a magnet with instrumented flux return (IFR) consisting of layers of iron interspersed with resistive plate chambers or limited streamer tubes. The data sample has an integrated luminosity of 348 fb^{-1} collected at the $\Upsilon(4S)$ resonance, which corresponds to $(383 \pm 4) \times 10^6 B\bar{B}$ pairs. It is assumed that the $\Upsilon(4S)$ decays equally to neutral and charged B -meson pairs. In addition, 37 fb^{-1} of data collected 40 MeV below the $\Upsilon(4S)$ resonance are used for background studies.

Candidate B mesons are reconstructed from four tracks that are consistent with originating from a common decay point within the PEP-II luminous region. Each of the four tracks is required to have at least 12 hits in the drift chamber and a transverse momentum greater than $100 \text{ MeV}/c$. The tracks are identified as either pion or kaon candidates, with protons vetoed, using Cherenkov-angle information and ionization energy-loss rate measurements (dE/dx). The efficiency for kaon selection is approximately 80%, including geometric acceptance, while the probability of misidentification of pions as kaons is below 5% up to a laboratory momentum of $4 \text{ GeV}/c$. Muons are rejected using information predominantly from the IFR. Furthermore, the tracks are required to fail an electron selection based on their ratio of energy in the calorimeter to momentum in the drift chamber, shower shape in the calorimeter, dE/dx , and Cherenkov-angle information.

To characterize signal events, three kinematic variables and one event-shape variable are used. The first kinematic variable, ΔE , is the difference between the center-of-mass (c.m.) energy of the B candidate and $\sqrt{s}/2$, where \sqrt{s} is the total c.m. energy. The second is the beam-energy-substituted mass $m_{\text{ES}} = \sqrt{(s/2 + \mathbf{p}_i \cdot \mathbf{p}_B)^2/E_i^2 - \mathbf{p}_B^2}$, where \mathbf{p}_B is the B momentum and (E_i, \mathbf{p}_i) is the four-momentum of the $\Upsilon(4S)$ in

the laboratory frame. The third kinematic variable is the $K^+\pi^-$ invariant mass, $m_{K^*\pi^-}$, used to identify K^{*0} candidates. B Candidates are required to be in the ranges $|\Delta E| < 0.1$ GeV, $5.2500 < m_{\text{ES}} < 5.2889$ GeV/ c^2 , and $0.776 < m_{K^*\pi^-} < 0.996$ GeV/ c^2 . The event-shape variable is a Fisher discriminant \mathcal{F} [9], constructed as a linear combination of the absolute value of the cosine of the angle between the B candidate momentum and the beam axis, the absolute value of the cosine of the angle between the thrust axis of the decay products of the B candidate and the beam axis, and the zeroth and second angular moments of energy flow about the thrust axis of the reconstructed B .

Continuum quark production ($e^+e^- \rightarrow q\bar{q}$, where $q = u, d, s, c$) is the dominant source of background. It is suppressed using another event-shape variable, $|\cos\theta_T|$, which is the absolute value of the cosine of the angle θ_T between the thrust axis of the selected B candidate and the thrust axis of the rest of the event. For continuum background, the distribution of $|\cos\theta_T|$ is strongly peaked towards 1.0 whereas the distribution is essentially flat for signal events. Therefore, the relative amount of continuum background is reduced by requiring $|\cos\theta_T| < 0.8$.

Monte Carlo (MC) events that are at least a 1000 times the number expected in data are used to study background from other B -meson decays. The largest B -background for $B^0 \rightarrow K^{*0}\pi^+\pi^-$ candidates comes from decays including charmonium mesons, such as $J/\psi K^{*0}$, $\chi_{c0} K^{*0}$ and $\psi(2S) K^{*0}$, where charmonium decays to $\mu^+\mu^-$ are misidentified as decays to $\pi^+\pi^-$, or where the charmonium decays directly to $\pi^+\pi^-$. These background events are removed by vetoing reconstructed $\pi^+\pi^-$ masses in the ranges $3.00 < m_{\pi^+\pi^-} < 3.20$ GeV/ c^2 , $3.35 < m_{\pi^+\pi^-} < 3.50$ GeV/ c^2 and $3.60 < m_{\pi^+\pi^-} < 3.78$ GeV/ c^2 , corresponding to the J/ψ , χ_{c0} and $\psi(2S)$ meson masses, respectively. For $B^0 \rightarrow K^{*0}K^+K^-$ candidates, $\chi_{c0} K^{*0}$ events are removed by rejecting events with a reconstructed invariant mass in the range $3.32 < m_{K^+K^-} < 3.53$ GeV/ c^2 .

Potential charm contributions from $B^0 \rightarrow D^-(\rightarrow K^{*0}h_2^-)h_1^+$ events are removed from corresponding $B^0 \rightarrow K^{*0}h_1^+h_2^-$ candidates by vetoing events with a reconstructed $K^{*0}h_2^-$ invariant mass in the range $1.83 < m_{K^*h} < 1.91$ GeV/ c^2 . To remove background from D^0 mesons, a veto is applied to any $K\pi$ pair with an invariant mass in the range $1.83 < m_{K\pi} < 1.91$ GeV/ c^2 for each $B^0 \rightarrow K^{*0}h_1^+h_2^-$ decay. Studies of MC events show the largest remaining charmed background is $B^0 \rightarrow D^-(\rightarrow K^{*0}\pi^-)\pi^+$, with 11% passing the veto. Surviving charmed events have a reconstructed D mass outside the veto range as a result of using a wrong π^- or K^+ candidate that is incorrectly selected from the other B decay in the event.

A fraction of events for all decay modes have more than one B^0 candidate reconstructed. For those events,

the candidate with the smallest χ^2 of the fitted B decay vertex is selected. Studies of MC events show the selection of $B^0 \rightarrow K^{*0}\pi^+K^-$ events produce the largest number of multiple candidates, in 21% of events, where for these multiple candidates the correct one is selected 65% of the time.

After all requirements have been applied, there are five main sources of remaining B background: two-body decays proceeding via a charmonium meson; two and three-body decays proceeding via a D meson; combinatorial background from three unrelated particles ($K^{*0}h_1^+h_2^-$); charmless two or four-body B decays with an extra or missing particle and three-body decays with one or more particles misidentified. Along with selection efficiencies obtained from MC simulation, existing branching fractions for these modes [10, 11] are used to estimate their background contributions that are included in fits to data.

In order to extract the signal event yield for the channel under study, an unbinned extended maximum likelihood fit is used. The likelihood function for N candidates is

$$\mathcal{L} = \frac{1}{N!} \exp\left(-\sum_{i=1}^M n_i\right) \prod_{j=1}^N \left(\sum_{i=1}^M n_i P_i(\vec{\alpha}, \vec{x}_j)\right), \quad (2)$$

where $M = 3$ is the number of hypotheses (signal, continuum background, and B -background), n_i is the number of events for each hypothesis determined by maximizing the likelihood function, and $P_i(\vec{\alpha}, \vec{x}_j)$ is a probability density function (PDF) with the parameters $\vec{\alpha}$ and $\vec{x} = (m_{\text{ES}}, \Delta E, \mathcal{F} \text{ and } m_{K^*\pi^-})$. The PDF is a product $P_i(\vec{\alpha}, \vec{x}) = P_i(\vec{\alpha}_{m_{\text{ES}}}, m_{\text{ES}}) \times P_i(\vec{\alpha}_{\Delta E}, \Delta E) \times P_i(\vec{\alpha}_{\mathcal{F}}, \mathcal{F}) \times P_i(\vec{\alpha}_{m_{K^*\pi^-}}, m_{K^*\pi^-})$. Studies of MC simulations show that correlations between these variables are small for the signal and continuum background hypotheses. However, for B -background, correlations are observed between m_{ES} and ΔE , which are taken into account by forming a 2-dimensional PDF for these variables.

The parameters for signal and B -background PDFs are determined from MC simulation. All continuum background parameters are allowed to vary in the fit, in order to help reduce systematic effects from this dominant event type. Sideband data, defined to be in the region $0.1 < \Delta E < 0.3$ GeV and $5.25 < m_{\text{ES}} < 5.29$ GeV/ c^2 , as well as data collected 40 MeV below the $\Upsilon(4S)$ resonance, are used to model the continuum background PDFs. For the m_{ES} PDFs, a Gaussian distribution is used for signal, a threshold function [12] for continuum and a two-dimensional histogram for B -background. For the ΔE PDFs, a sum of two Gaussian distributions with distinct means is used for the signal, a first-order polynomial for the continuum background and a two-dimensional histogram is used for B -background. The signal, continuum and B -background \mathcal{F} PDFs are described using a sum of two Gaussian distributions with distinct means

and widths. Finally, for m_{K^*0} PDFs, a sum of the Breit-Wigner function and a first-order polynomial describes the signal, continuum, and B -background distributions. The first-order polynomial component of the m_{K^*0} PDFs is used to model misreconstructed events in signal and background. Within the m_{K^*0} fit range, there is also the possibility of B -background contributions from nonresonant and higher K^*0 resonances, which are modeled in the fit using the LASS parameterization [13, 14]. The contribution from this background is estimated by extrapolating a $K\pi$ invariant mass projection fitted in a higher-mass region ($0.996 < m_{K^*0} < 1.53$ GeV/ c^2) into the signal region. This estimated background is modeled in the final fit into the signal region, and assumes there are no interference effects between the $K\pi$ background and the $K^*0(892)$ signal.

Branching fractions \mathcal{B} are usually calculated with the equation $\mathcal{B} = n_{\text{sig}} / (N_{B\bar{B}} \times \epsilon)$, where n_{sig} is the fitted number of signal events n_1 , ϵ is the average signal efficiency obtained from MC simulation and $N_{B\bar{B}}$ is the total number of $B\bar{B}$ events. For the $B^0 \rightarrow K^*0 h_1^+ h_2^-$ branching fraction, the average efficiency cannot be taken directly from MC events. This is due to the efficiency variations across the Dalitz plane and because the distribution of events in the Dalitz plane is a priori unknown. To calculate the branching fraction, a weight is assigned to each event j as

$$\mathcal{W}_j = \frac{\sum_i V_{1,i} P_i(\vec{\alpha}, \vec{x}_j)}{\sum_k n_k P_k(\vec{\alpha}, \vec{x}_j)}, \quad (3)$$

where $V_{1,i}$ is the row of the covariance matrix associated with the n_1 parameter, obtained from the fit [15]. This procedure is effectively a background subtraction where the weights have the property $\sum_j \mathcal{W}_j = n_{\text{sig}}$. The branching fraction is then calculated as $\mathcal{B} = \sum_j \mathcal{W}_j / (\epsilon_j \times N_{B\bar{B}})$, where ϵ_j (a function of $m_{K^*0 h_1^+}^2$, $m_{K^*0 h_2^-}^2$ and the $K^*0 \rightarrow K^+ \pi^-$ decay helicity angle) varies across phase space and is simulated in bins using over eight million MC events for each channel. The sizes of the bins are optimized to provide continuous coverage of the efficiency distribution.

Figure 2 shows the fitted m_{ES} projections for the $B^0 \rightarrow K^*0 K^+ K^-$, $B^0 \rightarrow K^*0 \pi^+ K^-$, $B^0 \rightarrow K^*0 K^+ \pi^-$, and $B^0 \rightarrow K^*0 \pi^+ \pi^-$ candidates, while the fitted signal yields, measured branching fractions, upper limits and asymmetries are shown in Table I. The candidates in Fig. 2 are signal-enhanced, with a requirement on the probability ratio $\mathcal{P}_{\text{sig}} / (\mathcal{P}_{\text{sig}} + \mathcal{P}_{\text{bkg}})$, optimized to enhance the visibility of potential signal, where \mathcal{P}_{sig} and \mathcal{P}_{bkg} are the signal and the total background probabilities, respectively (computed without using the variable plotted). The 90% confidence level (C.L.) branching fraction upper limit (\mathcal{B}_{UL}) is determined by integrating the likelihood distribution (with systematic uncertainties included) as a function of the branching fraction from 0 to

\mathcal{B}_{UL} , so that $\int_0^{\mathcal{B}_{\text{UL}}} \mathcal{L} d\mathcal{B} = 0.9 \int_0^\infty \mathcal{L} d\mathcal{B}$. The signal significance S is defined as $\sqrt{2\Delta \ln \mathcal{L}}$, where $\Delta \ln \mathcal{L}$ represents the change in log-likelihood (with systematic uncertainties included) between the maximum value and the value when the signal yield is set to zero.

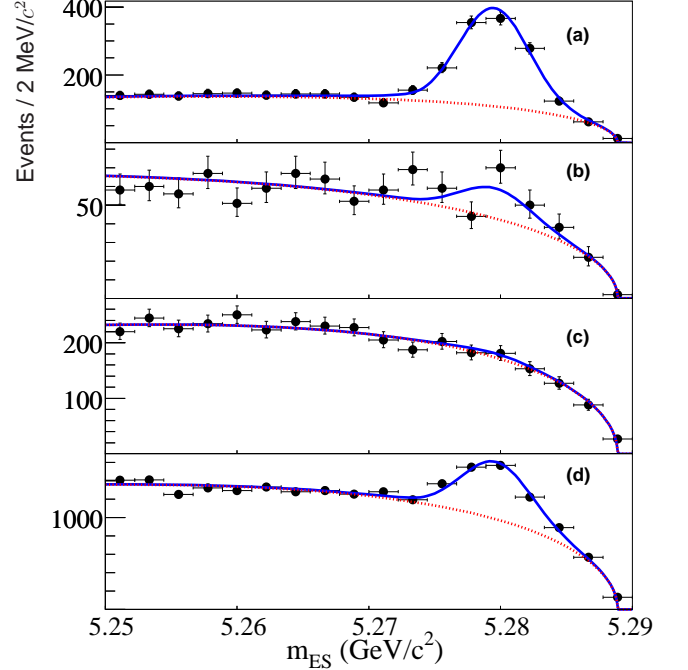


FIG. 2: Maximum likelihood fit projections of m_{ES} for signal-enhanced samples of charmless $B^0 \rightarrow K^*0 h_1^+ h_2^-$ candidates. The dashed line is the fitted background PDF while the solid line is the sum of the signal and background PDFs. The points indicate the data. The plot shows projections for (a) $B^0 \rightarrow K^*0 K^+ K^-$, (b) $B^0 \rightarrow K^*0 \pi^+ K^-$, (c) $B^0 \rightarrow K^*0 K^+ \pi^-$ and (d) $B^0 \rightarrow K^*0 \pi^+ \pi^-$.

Contributions to the branching fraction systematic uncertainty are shown in Table II. Errors due to tracking efficiency are assigned by comparing control channels in MC simulation and data. The error in the efficiency is due to limited MC statistics of the signal event samples. The number of $B\bar{B}$ events is calculated with an uncertainty of 1.1%. To calculate errors due to the fit procedure, a large number of MC samples are used, containing the numbers of signal and continuum events measured in data and the estimated number of exclusive B -background events. The differences between the generated and fitted values are used to estimate small fit biases (see Table II) that are a consequence of correlations between fit variables. These biases are applied as corrections to obtain the final signal yields, and half of the correction is added as a systematic uncertainty. The uncertainty of the B -background contribution to the fit is estimated by varying the known branching fractions within their errors. Each background is var-

TABLE I: Signal yields, B -background yields (B bkg), efficiencies, and branching fractions (B), measured using $K^+\pi^-h_1^+h_2^-$ events. Fit bias corrections are applied to the signal yields and branching fractions. The first error is statistical and the second error is systematic. The efficiencies take into account $\mathcal{B}(K^{*0} \rightarrow K^+\pi^-) = 2/3$, assuming isospin symmetry. The significance S is shown for $B^0 \rightarrow K^{*0}\pi^+K^-$ and $B^0 \rightarrow K^{*0}K^+\pi^-$ and the branching fraction upper limit at 90% C.L. is shown for $B^0 \rightarrow K^{*0}K^+\pi^-$. Asymmetries (\mathcal{A}_{K^*hh}) are reported only for the channels with significant yields.

Mode	Total Events	B bkg	Signal Yield	Signal Efficiency(%)	\mathcal{B} ($\times 10^{-6}$)	\mathcal{B}_{UL} ($\times 10^{-6}$)	S (σ)	Asymmetry (\mathcal{A}_{K^*hh})
$B^0 \rightarrow K^{*0}K^+K^-$	11185	221	984 ± 46	9.3	$27.5 \pm 1.3 \pm 2.2$	—	> 10	$0.01 \pm 0.05 \pm 0.02$
$B^0 \rightarrow K^{*0}\pi^+K^-$	53991	276	183 ± 42.4	10.4	$4.6 \pm 1.1 \pm 0.8$	—	5.3	$0.22 \pm 0.33 \pm 0.20$
$B^0 \rightarrow K^{*0}K^+\pi^-$	16248	372	18.8 ± 29.4	9.8	$0.5 \pm 0.8 \pm 0.5$	2.2	0.9	—
$B^0 \rightarrow K^{*0}\pi^+\pi^-$	100750	1701	2019 ± 108	9.7	$54.5 \pm 2.9 \pm 4.3$	—	> 10	$0.07 \pm 0.04 \pm 0.03$

ied individually and the effect on the fitted signal yield is added in quadrature as a contribution to the uncertainty. The higher K^{*0} background is varied by its uncertainty and the largest change to the signal yield is added as a systematic error. The uncertainty due to reconstructing the wrong $B^0 \rightarrow K^{*0}h_1^+h_2^-$ signal candidate as a consequence of K/π misidentification (for example $B^0 \rightarrow K^{*0}K^+K^-$ events being reconstructed as $B^0 \rightarrow K^{*0}\pi^+K^-$) is determined using MC events and added as a systematic uncertainty. We compute uncertainties and corrections to MC using the high statistics calibration channel $B^0 \rightarrow D^-(\rightarrow K^{*0}\pi^-)\pi^+$. Over 7000 events are selected using the $B^0 \rightarrow K^{*0}\pi^+\pi^-$ selection criteria and requiring the reconstructed $K^{*0}\pi^-$ invariant mass to be in the range $1.84 < m_{K^{*0}\pi^-} < 1.88$ GeV/ c^2 . The uncertainty due to PDF modeling is estimated from the calibration channel and by varying the PDFs according to the precision of the parameters obtained from the calibration channel fit to data. In order to take correlations between parameters into account, the full correlation matrix is used when varying the parameters. All PDF parameters that are originally fixed in the fit are then varied in turn, and each difference from the nominal fit is combined in quadrature and taken as a systematic contribution.

Interference effects between the $K^{*0}(892)$ and spin-0 final states (nonresonant and $K_0^{*0}(1430)$) integrate to zero if the acceptance of the detector and analysis is uniform; the same is true of the interference between the $K^{*0}(892)$ and spin-2 final states ($K_2^{*0}(1430)$). Studies of MC events show the efficiency variations are small enough to make these interference effects insignificant. The integrated interference between $K^{*0}(892)$ and other spin-1 amplitudes such as $K^{*0}(1410)$ is in principle nonzero, but in practice is negligible due to the small branching fraction of $K^{*0}(1410) \rightarrow K^+\pi^-$ ($6.6 \pm 1.3\%$ [11]) and the fact that the $K\pi$ mass lineshapes have little overlap.

The CP -violating asymmetries for the decays $B^0 \rightarrow K^{*0}K^+K^-$, $B^0 \rightarrow K^{*0}\pi^+K^-$, and $B^0 \rightarrow K^{*0}\pi^+\pi^-$ are shown in Table I and are consistent with zero. The background asymmetries $\mathcal{A}_{K^*KK}^{\text{bkg}}$, $\mathcal{A}_{K^*K\pi}^{\text{bkg}}$, and $\mathcal{A}_{K^*\pi\pi}^{\text{bkg}}$, which

TABLE II: Summary of systematic uncertainty contributions to the branching fraction measurements $B^0 \rightarrow K^{*0}h_1^+h_2^-$. Multiplicative errors are shown as a percentage of the branching fraction and additive errors are shown in events. The final row shows the total systematic error on the branching fraction.

Error source	$K^{*0}K^+K^-$ error	$K^{*0}\pi^+K^-$ error	$K^{*0}K^+\pi^-$ error	$K^{*0}\pi^+\pi^-$ error
Multiplicative errors (%)				
Tracking	2.0	2.0	2.0	2.0
Efficiency	3.8	3.9	3.9	4.2
No. of $B\bar{B}$	1.1	1.1	1.1	1.1
Tot. mult.(%)	4.4	4.5	4.5	4.7
Additive errors (events)				
Fit Bias	14	10	2	43
B -background	17	13	13	26
Higher K^{*0} bkg	58	0	0	118
Signal mis-id	0	6	11	0
PDF params.	20	26	4	19
Tot. add. (events)	65	31	18	130
Total (10^{-6})	2.2	0.8	0.5	4.3

are expected to be consistent with zero, are measured to be 0.017 ± 0.010 , 0.007 ± 0.004 , and 0.0018 ± 0.0033 , respectively.

The systematic error on $\mathcal{A}_{K^*h_1h_2}$ is calculated by considering contributions due to track finding, fit biases, B -background uncertainties and particle interaction asymmetries. The error due to fit biases is found to be negligible. Tracking efficiency uncertainties are assigned by comparing the total number of reconstructed tracks for control channels in data and MC simulation. The interaction asymmetry of matter and antimatter with the detector is studied using MC, where biases between -0.01 and -0.03 are observed and applied as corrections to the data. The uncertainty on the correction, obtained from the calibration channel asymmetry difference between MC and data, is added as a systematic uncertainty. The contri-

bution from B -background is calculated by varying the number of expected events within errors and by conservatively assuming a large CP -violating asymmetry of ± 0.2 , as there are no available measurements for these decays.

In summary, we analyze $K^+\pi^-h_1^+h_2^-$ final states to obtain branching fraction and CP -asymmetry measurements for the decays $B^0 \rightarrow K^{*0}K^+K^-$, $B^0 \rightarrow K^{*0}\pi^+K^-$ and $B^0 \rightarrow K^{*0}\pi^+\pi^-$. We find the results to be consistent with the Standard Model, observing the decay $B^0 \rightarrow K^{*0}\pi^+K^-$ with a 5.3 standard deviation significance and placing an upper limit on the branching fraction $B^0 \rightarrow K^{*0}K^+\pi^-$. We find no evidence for CP -violation.

We are grateful for the excellent luminosity and machine conditions provided by our PEP-II colleagues, and for the substantial dedicated effort from the computing organizations that support *BABAR*. The collaborating institutions wish to thank SLAC for its support and kind hospitality. This work is supported by DOE and NSF (USA), NSERC (Canada), CEA and CNRS-IN2P3 (France), BMBF and DFG (Germany), INFN (Italy), FOM (The Netherlands), NFR (Norway), MIST (Russia), MEC (Spain), and STFC (United Kingdom). Individuals have received support from the Marie Curie EIF (European Union) and the A. P. Sloan Foundation.

* Deceased

† Now at Tel Aviv University, Tel Aviv, 69978, Israel

‡ Also with Università di Perugia, Dipartimento di Fisica, Perugia, Italy

§ Also with Università della Basilicata, Potenza, Italy

¶ Also with Universitat de Barcelona, Facultat de Física, Departament ECM, E-08028 Barcelona, Spain

- [1] N. Cabibbo, Phys. Rev. Lett. **10**, 531 (1963); M. Kobayashi and T. Maskawa, Prog. Theor. Phys. **49**, 652 (1973).
- [2] B. Aubert *et al.* (*BABAR* Collaboration), Phys. Rev. Lett. **91**, 171802 (2003).
- [3] B. Aubert *et al.* (*BABAR* Collaboration), Phys. Rev. Lett. **97**, 201801 (2006).
- [4] K. F. Chen *et al.* (Belle Collaboration), Phys. Rev. Lett. **94**, 221804 (2005).
- [5] H. Albrecht *et al.* (ARGUS Collaboration), Phys. Lett. B **262**, 148 (1991).
- [6] B. Aubert *et al.* (*BABAR* Collaboration), Phys. Rev. D **74**, 051104 (2006).
- [7] The use of charge-conjugate modes is implied throughout this paper unless otherwise noted.
- [8] B. Aubert *et al.* (*BABAR* Collaboration), Nucl. Instr. Meth. A **479** 1 (2002).
- [9] R. A. Fisher, Ann. Eugenics **7**, 179 (1936); G. Cowan, *Statistical Data Analysis*, 51 (Oxford University Press, 1998).
- [10] The Heavy Flavor Averaging Group (HFAG), <http://www.slac.stanford.edu/xorg/hfag/rare/winter07/charmless/index.html>.
- [11] W. M. Yao *et al.* (Particle Data Group), J. Phys. G **33**, 1 (2006).
- [12] H. Albrecht *et al.* (ARGUS Collaboration), Z. Phys. C **48**, 543 (1990).
- [13] D. Aston *et al.*, Nucl. Phys. B **296**, 493 (1988).
- [14] B. Aubert *et al.* (*BABAR* Collaboration), Phys. Rev. D **72**, 072003 (2005).
- [15] M. Pivk and F. R. Le Diberder, Nucl. Instr. Meth. A **555**, 356 (2005).